
ORIGINAL ARTICLE

Field of the paper

Numerical Solution of Schrodinger Equation for Rotating Morse Potential using Matrix Methods with Fourier Sine Basis

Aditi Sharma and O.S.K.S. Sastri¹

¹Department of Physical and Astronomical Sciences, Central University of Himachal Pradesh(CUHP), Dharamshala, H.P.,176215, India(Bharat)

Correspondence

O.S.K.S. Sastri, Department of Physical and Astronomical Sciences, Central University of Himachal Pradesh(CUHP), Dharamshala, H.P.,176215, India(Bharat)
Email: sastri.osks@hpcu.ac.in

Funding information

In this paper, an elegant and easy to implement numerical method using matrix mechanics approach is proposed, to solve the time independent Schrodinger equation (TISE) for Morse potential. It is specifically applied to non-homogeneous diatomic molecule HCl to obtain its rotating-vibrator spectrum. While matrix diagonalization technique is utilised for solving TISE, model parameters for Morse potential are optimized using variational Monte-Carlo (VMC) approach by minimizing χ^2 - value. Thus, validation with experimental vibrational frequencies is completely numerical based with no recourse to analytical solutions. The ro-vibrational spectra of HCl molecule obtained using the optimized parameters through VMC have resulted in least χ^2 - value as compared to those determined using best parameters from multiple regression analysis of analytical expressions. Numerical algorithm for solving the Hamiltonian matrix has been implemented utilizing Free Open Source Software (FOSS) Scilab and simulation results are matching well with those obtained using analytical solutions from Nikiforov-Uvarov (NU) method and asymptotic iteration method (AIM).

Keywords – Morse potential, Matrix method, Variational Monte Carlo (VMC), Scilab.

Abbreviations: ABC, a black cat; DEF, doesn't ever fret; GHI, goes home immediately.

1 | INTRODUCTION

Obtaining the bound state solutions of time independent Schrodinger equation (TISE) has remained one of the central aspects of quantum mechanics and its application to atomic, molecular, nuclear and solid state physics. All these physical systems are modeled using various potentials that typically have an attractive nature that dies down zero reasonably fast and a repulsive core at short distances. A large number of exponential type potentials such as Rosen-Morse((Zhang2012), (Ikhdair 2010)), Manning-Rosen ((Manning1933), (Manning1933), (Qiang2007), (Ikhdair2008)), Kratzer(Berkdemir2006), (Berkdemir2007), (Ikhdair2008)) and other multi-parameter potentials ((Egrifes2000), (Jia2004)) are used in both molecular and nuclear physics. Among all these, Morse potential has proved to be one of the most successful in explaining rotational and vibrational structure of diatomic molecules (Rosen1932), even till date.

Many analytical methods have been proposed to solve TISE for obtaining its exact energies and corresponding wave-functions. The recent analytical techniques like super-symmetry quantum mechanics (SUSYQM) ((Levai1992), (Morales2004)), Nikiforov-Uvarov ((Ikhdair1992), (Nikiforov2004), (Berkdemir2005)), point canonical transformations (De1992), Pekeris-type approximation (Zhang2011), Taylor expansion(Chou2011) Lie algebraic method(Palma2011) and Asymptotic Iteration Method(AIM) have been very successful in solving TISE for complex potential functions which were beyond the reach of regular solutions using Frobenius method or special functions approach. The eigen energies of Morse potential with the use of Perkeris approximation are obtained for Morse potential using AIM(Al-Dossary 2007) and SUSYQM (Hassanabadi 2012). Also, bound state solutions of D-dimensional Schrodinger equation are determined for class of exponential type Hulthen, Manning-Rosen, Eckart and Deng Fan potentials(Pena 2014). Likewise, various numerical methods have been implemented to solve second order differential equation which consists of $1/N$ expansion ((Qiang2007a),(Ikhdair2003)), finite element analysis (Xu2009), Runge-Kutta techniques ((Van de Vyver 2005),(Anastassi 2005)), homotopy analysis((Alomari 2009),(Jia 2010)) and so on. Recently, Hassanabadi et. al. followed both SUSYQM and finite difference methods to obtain reliable solution of radial Schrodinger equation for Hua potential which is similar to Eckart, Manning-Rosen, or Morse potentials.

In this paper, TISE is solved for obtaining ro-vibrational spectrum of Morse potential using matrix method technique proposed by Marsiglio et.al., (Marsiglio 2009). They first implemented it for harmonic oscillator potential(Marsiglio 2009) and then extended it further for central potentials such as spherical well, Coulomb and Yukawa potentials (Jugdutt 2013). The central idea of the method is to embed the potential of interest within an infinite square potential, whose solutions which are sine eigen-functions, are utilised as basis for obtaining the matrix form of TISE to be solved using an eigen solver. Following this, we have recently applied it to obtain single particle neutron and proton energies using nuclear shell model with Woods-Saxon and spin-orbit interactions (Sharma 2020). Also, a study of square well potential (Sastri 2019), pure quartic and anharmonic oscillators (Sharma 2020a), and vibrational spectrum of diatomic molecules (Sastri 2020) have been undertaken in simple worksheet environment in Gnumeric software. Here, we extend the study to obtaining the rotational fine structure of the vibrational spectrum. One of the important features of this study involves optimising the model parameters using VMC technique. The χ^2 -value between the simulated and experimental frequencies (which is akin to least squares minimisation) is reduced in a variational sense, by randomly allowing each of the parameters to be varied successively in every iteration, till the required accuracy is achieved. The paper is structured as follows.

First, in section 2, the need for modeling the interaction by Morse type function has been reinforced by obtaining the electronic ground state energy for different distances from first principle calculations. This is followed by section 3 that deals with preparation of system for simulation, by briefly discussing the numerical technique being used and rephrasing the problem in appropriate units. Then, the steps for implementation are clearly specified. Following which, testing of code and optimising of algorithm parameters, for a known set of model parameters obtained from fitting

experimental data using analytical expressions, is presented. In section 4, the procedure for optimisation of model parameters using VMC approach is deliberated and the results are generated in the process. The simulation results for vibrational spectrum consisting of its rotational fine structure have been validated with experimental values obtained from FTIR (Polik 1999). Finally, the optimized model parameters using VMC have been substituted into analytical expressions for energies from NU and AIM methods, to obtain the rotational energies within each vibrational level. A comparison with simulation results, shows perfect match between all the three approaches.

2 | MODELING DIATOMIC MOLECULE AS A VIBRATING ROTATOR:

In this section, we first discuss aspects of modeling such as description, formulation and ramification stages involved in solving for vibrational and rotational energies of a diatomic molecule.

2.1 | Description

The rotational and vibrational motions of a linear non-homogeneous diatomic molecule of AB-type consisting of nuclei N_A & N_B , and n electrons can be described by considering three types of Coulomb interactions:

1. $e^- - e^-$ repulsion:

$$V_{e^- - e^-} = \sum_{i=1}^{n-1} \sum_{j=i+1}^n \frac{e^2}{4\pi\epsilon_0 r_{ij}} \quad (1)$$

where $r_{ij} = |\bar{r}_i - \bar{r}_j|$ is the distance between i^{th} e^- and j^{th} e^- .

2. $N_A - N_B$ repulsion:

$$V_{N-N} = \frac{Z_A Z_B e^2}{4\pi\epsilon_0 R_{AB}} \quad (2)$$

where $R_{AB} = |\bar{R}_A - \bar{R}_B|$ is distance between the nuclei, Z_A and Z_B are their respective charges.

3. $e^- - N$ attraction:

$$V_{e^- - N} = \sum_{i=1}^N \left(\frac{-Z_A e^2}{4\pi\epsilon_0 |\bar{r}_i - \bar{R}_A|} + \frac{-Z_B e^2}{4\pi\epsilon_0 |\bar{r}_i - \bar{R}_B|} \right) \quad (3)$$

and is dependent on the distance between i^{th} e^- and corresponding nuclei.

2.2 | Formulation:

The Hamiltonian for the diatomic molecule is given by

$$H = \left(-\frac{\hbar^2}{2m_A} \frac{\partial^2}{\partial \bar{R}_A^2} - \frac{\hbar^2}{2m_B} \frac{\partial^2}{\partial \bar{R}_B^2} \right) + \left(-\frac{\hbar^2}{2m_e} \sum_{i=1}^N \frac{\partial^2}{\partial \bar{r}_i^2} \right) + V_{N-N} + V_{e^- - N} + V_{e^- - e^-} \quad (4)$$

Using Born Oppenheimer (BO) approximation, wave-function $\Psi(\vec{r}_i, \vec{R}_A, \vec{R}_B)$ as product of e^- and nuclear wave-functions $\phi_e(\vec{r}_i; \vec{R}_A, \vec{R}_B)$ and $\chi_N(\vec{R}_A, \vec{R}_B)$ respectively, and using separation of variable, one obtains the TISE for e^- s and nuclear vibrational and rotational motion as

$$-\frac{\hbar^2}{2m_e} \sum_{i=1}^N \frac{\partial^2 \phi_e}{\partial \vec{r}_i^2} + [V_{e-N} + V_{e-e^-} + V_{NN}(R_{AB})] \phi_e = E_e \phi_e \quad (5)$$

and

$$\left(-\frac{1}{2m_A} \frac{\partial^2}{\partial \vec{R}_A^2} - \frac{1}{2m_B} \frac{\partial^2}{\partial \vec{R}_B^2} + U_e(R_{AB}) \right) \chi_N(\vec{R}_A, \vec{R}_B) = E \chi_N(\vec{R}_A, \vec{R}_B) \quad (6)$$

where $U_e(R_{AB})$ is the potential function obtained by solving electronic TISE for its ground state energy $E_e(\vec{r}_i; \vec{R}_A, \vec{R}_B)$ for different inter-nuclear distances R_{AB} . When TISE is transformed, using $(\vec{R}_A, \vec{R}_B) \rightarrow (\vec{R}_{CoM}, \vec{R})$, into a one-body problem describing the reduced mass μ of the molecule, R_{AB} becomes the relative distance co-ordinate $R = |\vec{R}|$ w.r.t center of mass co-ordinate \vec{R}_{CoM} .

Using FOSS such as Gamess, a code for obtaining ground state energy of the molecule using Hartree-Fock (HF) or density functional theory (DFT), typical functional form of $U_e(R)$ is obtained (see Fig.1) and it has a form as proposed by Morse (Morse 1932), given by

$$U_e(R) = D_e \left(e^{-2\alpha x} - 2e^{-\alpha x} \right) \quad (7)$$

Here $x = \frac{(R-R_e)}{R_e}$ and $\alpha = bR_e$, where $R = R_e$ is the equilibrium bond length at which the potential attains a minima. Parameter α describes the shape of the curve and is a characteristic that is different for various molecules. With increasing R , the potential reaches a constant value D_e , as a result of dissociation of the molecule. Since the potential is dependent only on distance R , it is central in character and spherical polar co-ordinates are appropriate choice for reference system.

Once again invoking the BO approximation, in this case, to separate out the vibrational and rotational wave-functions, one can obtain the radial equation describing the vibrations as (Struve 1989)

$$\frac{d^2 S(R)}{dR^2} + \frac{2\mu}{\hbar^2} \left[E - U_e(R) - \frac{J(J+1)\hbar^2}{2\mu R^2} \right] S(R) = 0 \quad (8)$$

So, an effective vibrational potential can be defined as $U(R) = U_e(R) + U_{cf}(R)$, where $U_{cf}(R) = \frac{J(J+1)\hbar^2}{2\mu R^2}$, represents the centrifugal potential that gives rise to the rotational levels of the molecule.

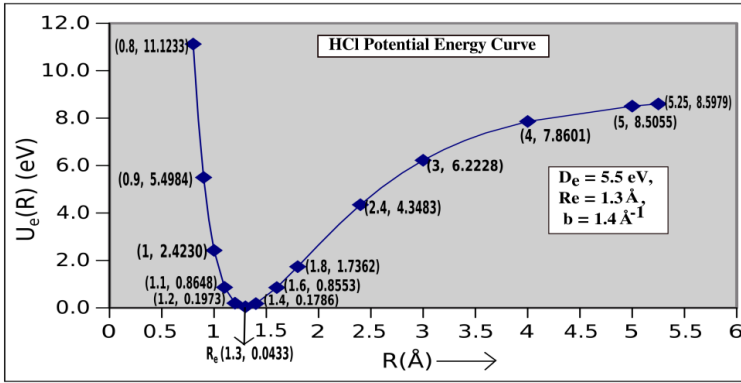


FIGURE 1 Graph of inter-nuclear distance R with ground state energy $U_e(R)$ of HCl molecule, obtained using FOSS Gamess

2.3 | Ramification:

The solution of TISE, as given by Eq. (8), can be obtained either analytically or numerically. The analytical solution is available for only studying vibrational spectra and energy values of vibrator-rotator is given by (Banwell 1972)

$$\varepsilon(\nu, J) = \bar{\omega}_e \left(\nu + \frac{1}{2}\right) - \bar{\omega}_e x_e \left(\nu + \frac{1}{2}\right)^2 + BJ(J+1)cm^{-1} \quad (9)$$

where $\bar{\omega}_e$ is oscillation frequency for anharmonic system at equilibrium and $\bar{\omega}_e x_e$ is anharmonicity constant which is always smaller than $\bar{\omega}_e$ and is positive. B is rotational constant given by

$$B = \frac{h}{8\pi^2 \mu R_e^2 c} cm^{-1}. \quad (10)$$

Emergent Properties:

The selection rules for transitions between the energy levels are obtained by utilising the eigen-functions of vibrator-rotator, which are the product of eigen-functions of vibrator and rotator respectively. Therefore, selection rules will be same as those for these two systems individually, (Struve 1989) i.e.

$$\begin{aligned} \Delta\nu &= \pm 1, \pm 2, \pm 3, \dots \\ \Delta J &= \pm 1 \end{aligned} \quad (11)$$

Vibrational Spectrum:

The analytical expressions for the first three vibrational frequencies corresponding to absorption from $\nu'' = 0$ and their experimental values for HCl, are given by (Banwell 1972)

$$\bar{\nu}_{0 \rightarrow 1} = \varepsilon_{\nu=1} - \varepsilon_{\nu=0} = \bar{\omega}_e(1 - 2x_e)cm^{-1} = 2886cm^{-1} \quad (12)$$

$$\bar{\nu}_{0 \rightarrow 2} = \varepsilon_{v=2} - \varepsilon_{v=0} = 2\bar{\omega}_e(1 - 3x_e)cm^{-1} = 5668cm^{-1} \quad (13)$$

$$\bar{\nu}_{0 \rightarrow 3} = \varepsilon_{v=3} - \varepsilon_{v=0} = 3\bar{\omega}_e(1 - 4x_e)cm^{-1} = 8347cm^{-1} \quad (14)$$

Vibrating Rotor Spectrum:

Now, including the rotational fine structure, for the main absorption, that is, $v'' = 0 \rightarrow v' = 1$, the wavenumbers corresponding to this transition are given by

$$\bar{\nu} = \bar{\omega}_0 + B_1J'(J' + 1) - B_0J''(J'' + 1)cm^{-1} \quad (15)$$

where $\bar{\omega}_0 = \bar{\omega}_e(1 - 2x_e)cm^{-1}$ is fundamental frequency and B_0 & B_1 are the rotational constants corresponding to vibrational states $v = 0$ and $v = 1$ respectively, with $B_0 > B_1$. The $\bar{\nu}$ can be determined from different values of J' and J'' . So, the rotational transitions $\Delta J = J' - J'' = +1$ gives one set of lines called as R branch, whereas those corresponding to $\Delta J = J' - J'' = -1$ are known as P branch.

3 | NUMERICAL SOLUTION OF VIBRATING ROTATOR

The main goal of this paper is to solve TISE given by Eq. (8) by numerical approach using matrix methods to obtain the energy eigen values and then apply variational Monte-Carlo (VMC) approach to optimize the model parameters such that frequencies obtained from simulation match the experimental ones by minimizing the χ^2 -value.

3.1 | Preparation of system for numerical solution

This stage involves three steps:

1. Choice of numerical technique: Schrodinger equation is often solved using Runge-kutta method, central divided difference or Numerov methods. In this paper, we focus on matrix diagonalization technique suggested by Marsiglio ((Dauphinee T. 2015),(Felipe 2016)) which is stable, highly efficient and gives accurate results as compared with the mentioned methods.

Matrix method: In this approach, the potential of interest $U_{vib}(R)$ is embedded within an infinite square well potential $[0, a_0]$. a_0 is the width, chosen to be certain cut-off radius, such that the characteristics of the potential are well represented. In this case, a_0 can be chosen as the value of R beyond which the potential value saturates to D_e and does not change any further significantly. This is equivalent to writing Eq. (8) as

$$\left[\frac{-\hbar^2}{2\mu} \frac{d^2 S(R)}{dR^2} + V_{inf}(R) + U^T(R) \right] S(R) = E S(R) \quad (16)$$

which can be rewritten as

$$\left[H_0 + U^T(R) \right] S(R) = E S(R) \quad (17)$$

where H_0 is the Hamiltonian of the infinite square well potential and $U^T(R)$ is the truncated potential defined in $[0, a_0]$. Expanding radial wave-function $S(R)$ in terms of infinite square eigen functions, chosen as basis functions

$$S(R) = \sum_{n=1}^{\infty} c_n \sqrt{\frac{2}{a_0}} \sin\left(\frac{n\pi R}{a_0}\right) \quad (18)$$

Eq. (17), can be transformed into the following matrix equation

$$\sum_{n=1}^{\infty} H_{mn} c_n = E c_m \quad \text{for } m = 1, 2, 3, \dots \quad (19)$$

where $H_{mn} = E_n^0 \delta_{mn} + V_{mn}$ is an infinite dimensional square symmetric matrix. E_n^0 are the energy eigen values of infinite square well Hamiltonian H_0 given by

$$E_n^0 = \frac{n^2 \pi^2 \hbar^2}{2\mu a_0^2} = n^2 E_1^0 \quad (20)$$

and V_{mn} is given by

$$V_{mn} = \int_0^{a_0} \sqrt{\frac{2}{a_0}} \sin\left(\frac{m\pi R}{a_0}\right) U^T(R) \sqrt{\frac{2}{a_0}} \sin\left(\frac{n\pi R}{a_0}\right) dR \quad (21)$$

We need to choose a finite number of basis functions, say N_0 for solving the problem numerically. The parameters a_0 and N_0 introduced into the technique are related to the algorithm, which are adjusted to ensure convergence and to match with expected results from experiment.

2. Rephrasing of units: In atomic and molecular physics, energy is measured in eV, distances in Å and frequencies in cm^{-1} . Therefore, these are chosen as the units for numerical calculations and the centrifugal and ground state energy terms are rephrased in eV as follows:

$$U_{c.f}(R) = \frac{J(J+1)\hbar^2}{2\mu R^2} = \frac{J(J+1)(\hbar c)^2}{2(\mu c^2)R^2 \times 10^6} \text{ eV} \quad (22)$$

where μ is reduced mass of diatomic molecule expressed in eV/c^2 and $\hbar c = 1973.29 eV\text{Å}$. and

$$E_1^0 = \frac{\pi^2 \hbar^2}{2\mu a_0^2} = \frac{\pi^2 (\hbar c)^2}{2(\mu c^2) a_0^2 \times 10^6} \text{ eV} \quad (23)$$

3. Discretizing the continuous variable: For doing simulation in computers, it is essential to discretize the continuous variable R with appropriate step-size and restrict it to a finite region of interest $[0, a_0]$.

3.2 | Implementation of Matrix Methods Algorithm:

1. Initialisation: The model parameters of Morse potential for HCl molecule to be initialised. In the NIST data compiled by Huber & Herzberg as well as in other references (Huber 1972), instead of Morse potential parameter values, the spectroscopic information of various diatomic molecules is given which includes constants like $\bar{\omega}_e$,

$\bar{\omega}_e x_e, R_e$. The formula to calculate D_e (Bernath 2020) and b (Zhang 2012) model values from data available is

$$D_e = \frac{\bar{\omega}_e^2}{4\bar{\omega}_e x_e} \text{ cm}^{-1} = \frac{\bar{\omega}_e^2}{4\bar{\omega}_e x_e} * 1.2397 \times 10^{-4} \text{ eV} \quad (24)$$

and

$$b = \sqrt{\frac{k_e}{2D_e}} = \sqrt{\frac{\mu\bar{\omega}_e^2}{2D_e}} \text{ \AA}^{-1} \quad (25)$$

where R_e can be calculated by using expression (Bernath 2020)

$$R_e = \sqrt{\frac{h}{8\pi^2\mu c B_e}} \text{ \AA} \quad (26)$$

parameters from multiple regression analysis of analytical expressions. Numerical algorithm for solving the Hamiltonian matrix has been implemented utilizing Free Open Source Software(FOSS) Scilab and simulation results are matching well with those obtained using analytical solutions from Nikiforov-Uvarov (NU) method and asymptotic iteration method (AIM).

where B_e is rotational constant corresponding to the separation R_e at the minimum of potential curve expressed in cm^{-1} .

2. **Potential definition:** The anharmonic Morse potential is chosen to be embedded within an infinite square well potential of width $a_0 = 6$ (where the potential saturates to constant value), and is given by

$$U_{vib}^T(R) = D_e(e^{-2\alpha x} - 2e^{-\alpha x}) + \frac{J(J+1)\hbar^2 c^2}{2\mu c^2 R^2} \quad (27)$$

3. **Defining H_{mn} matrix:** Hamiltonian matrix defined in Eq. (19) will be a square symmetric matrix consisting of diagonal and non-diagonal elements. Even though integrals can be solved analytically for $J = 0$ case, for the more general $J \neq 0$ that results in the rotational fine-structure require the matrix elements to be obtained using numerical integration. The diagonal and non-diagonal elements of H_{nm} matrix are obtained as

$$H_{nm} = \begin{cases} E_n^0 + \int_0^{a_0} \frac{2}{a_0} \left(\frac{1 - \cos(2n\pi R/a_0)}{2} \right) U_{vib}^T(R) dR, & \text{for } m = n \\ \int_0^{a_0} \frac{2}{a_0} \left(\frac{(1 - \cos((n-m)\pi R/a_0)) - (1 - \cos((n+m)\pi R/a_0))}{2} \right) U_{vib}^T(R) dR, & \text{for } m \neq n \end{cases} \quad (28)$$

For doing numerical integration, 'intspline' function is used.

4. **Obtaining eigen values:** In Scilab, 'spec' command is used for getting eigen values but the generated eigen values are in random order. So, 'gsort' is used for sorting the data in descending order. The obtained energies (in eV) are converted into wavenumbers by dividing all of them with a factor $hc = 1239.8419 * 10^{-7} \text{ eV cm}$. The vibrational frequencies can be obtained by taking appropriate energy differences as per selection rules.

The code for obtaining the vibrational frequencies from the energies obtained as eigen values of the h-matrix has been written in Scilab and is given in Appendix 1.

3.3 | Testing the correctness of code

Using the data obtained through multiple regression analysis, (Struve 1989) and the formulae given in Eqs. (24) to (26), the values of D_e , b and R_e are obtained as $5.346799eV$, 1.734985\AA^{-1} and 1.274808\AA respectively. On running the code, with $a_0 = 6$ and $N_0 = 50$, the first three pure vibrational frequencies ($J = 0$) corresponding to transitions from $v'' = 0$ to $v' = 1, 2, 3$ are obtained as $2911, 5824, 8730$ in cm^{-1} . These are not very close to the experimental values as specified in Eqs. (12)-(14). So, the number of basis functions, N_0 are increased in steps of 20 till 90, beyond which the resulting frequencies are, $\bar{\omega}_{10} = 2886, \bar{\omega}_{20} = 5668$ & $\bar{\omega}_{30} = 8346$ in cm^{-1} , converging to experimental values. This confirms that the code is implemented correctly to solve the TISE using matrix methods approach. Here, the model parameters for Morse potential are chosen based on fitting experimental data with analytical expressions obtained from solving the theoretical model. This is the usual procedure followed for performing numerical simulations. But, in this paper, the main intent is to establish numerical simulation as an independent methodology for solving the theoretical model without recourse to analytical solutions. Hence, we introduce in the next section, VMC optimization procedure for obtaining the model parameters that best validate the experimental observations.

3.4 | Optimization of Morse potential parameters using variational Monte Carlo approach

While Monte-Carlo approach involves varying the model parameters randomly by a small amount in each iteration, variational principle is invoked to minimize the χ^2 - value. So, over all VMC approach is a parallel methodology to least square minimisation procedure that is often employed with analytical expressions. The implementation algorithm for VMC is as follows:

1. Initialization: To begin with, the model parameters- D_e , b and R_e could be chosen based on some guess. Alternatively, the values could be chosen randomly or based on inputs from other techniques.

Here, for HCl molecule, equilibrium bond length $R_e = 1.2745$ known from rotational spectra is taken as its initial value. The parameters $D_e = 5$ and $b = 1$ are initial guesses, which are chosen some what close to data available from literature $D_e = 5.3$ and $b = 1.7439$.

2. Determination of simulation frequencies: Using these initial values, the TISE is solved using the matrix methods technique elucidated in the previous section and the energy eigen values are obtained. Since, each of the frequencies are a result of transitions to different energy levels, they can be regarded as independent degrees of freedom.

χ^2 - value: Hence, χ^2 can be calculated using following formula

$$\chi^2 = \sum_{i=1}^3 \frac{(v_i^{sim} - v_i^{exp})^2}{3} \quad (29)$$

This is akin to the idea of mean-square error. Store the value in a variable named *chisqrold*. **3. Monte-Carlo step:** Generate a random number ' r ' within an interval, say $[-l, l]$. Choose one parameter among the three, say D_e and change it to a new value by adding r to it. That is, say, $D_{e,new} = D_e + r$. Redetermine the simulated frequencies using this $D_{e,new}$ and obtain χ^2 - value. Store it in a new variable *chisqrnew*.

4. Variational Step: If *chisqrnew* is less than *chisqrold*, then the new value is accepted. That is D_e is updated as $D_{e,new}$, else old value of D_e is retained. That is nothing is done. If the condition is satisfied then one has to update the value of χ^2 as well. That is, $chisqrold = chisqrnew$.

5. Iterative Minimization: When the above steps are repeated for all parameters involved, then one iteration is completed. Then, the process is repeated over many iterations till the change in χ^2 is not remarkable, at which instance, size of interval is decreased by decreasing value of l . This allows for even smaller variations in the parameters. In

this way, one can reduce χ^2 till one achieves the desired level of accuracy to the appropriate decimal place in the parameters involved.

The VMC code, for minimization of χ^2 value for an interval $[-I, I]$, has been written in FOSS Scilab. It consists of inline documentation that makes it easy to understand and is available with authors.

4 | SIMULATION AND DISCUSSION OF RESULTS

The simulation results, obtained using model parameters obtained from multiple regression analysis data during the testing phase of the code, give a χ^2 -value of 0.245121 (Polik 1999).

One of the major contributions in this paper is to solve the TISE for Morse potential numerically without recourse to analytical solutions. Towards this goal, we now optimize the model parameters for the Morse potential to yield the best convergence to the experimental vibrational frequencies using the VMC approach. This has been implemented as three step process.

Step 1 Experimentally, from microwave spectra of molecules, the inter-nuclear distance, R_e is available to an accuracy of five decimal places as 1.27455Å (Huber 2013) and is kept constant initially. Now, one can begin with any random values of D_e and b as initial guesses but there is a possibility that it could lead the process either to get into a local minima or may result in a set of parameters that may not be those which are close to expected values obtained from analytical solutions. Also, starting with completely random guesses can increase the number of iterations to extremely large values thus increasing the computational time. It is always important to make calculated guesses from graphical procedures.

From observing Fig. 1, we have chosen the starting values for D_e and b to be 5 and 1 respectively. Now, the first three vibrational transition frequencies using matrix method are determined by converting the energy values obtained in eV for non-rotating Morse potential ($J = 0$) to wavenumbers (by dividing them with a factor of $hc = 1239.84193 * 10^{-7} eVcm$) and χ^2 -value is calculated with respect to experimental data available. This is stored in variable, named as *chisqrold*.

In each iteration, one by one, the parameters D_e and R_e are changed by a random value chosen in an interval $[-0.1, 0.1]$. Each time the program is run to determine the new frequencies and the corresponding χ^2 -value. This is stored in *chisqrnew*. The values of the parameters are updated if *chisqrnew* is less than *chisqrold*. This is repeated for 20,000 iterations. Using the obtained values of D_e and b as inputs, that is, as the new starting values, the program is run again for another 10,000 iterations. But, this time, the random value for making the change to the parameters is chosen from a smaller interval of $[-0.01, 0.01]$. This process of reducing the interval limits by a decimal place and running the program for 10,000 iterations is continued till the χ^2 -values has reached a value to less than 0.02. The results are shown in Table 1.

Step 2 Just to ensure that the variations in R_e are also accounted for, optimization procedure is repeated as before by allowing for changes in all three parameters in each iteration. That is, by starting from the last obtained parameters in the previous run, that is, $D_e = 5.347819 eV$, $b = 1.734941 \text{Å}^{-1}$, and $R_e = 1.27455 \text{Å}$. Each parameter is made to change by a random value picked in an interval $[-0.00001, 0.00001]$, (same as in the last run of previous step), in every iteration. At the end of 30,000 iterations, the χ^2 -value reduced to 0.019219, a change in the fourth decimal place, resulting in model parameter values as $D_e = 5.348363 eV$, $b = 1.734841 \text{Å}^{-1}$, and $R_e = 1.274187 \text{Å}$. This completes obtaining one single set of parameters using VMC technique.

Step 3 By proceeding in a similar fashion as discussed in previous two steps, four more sets have been completed and model parameters are determined for each set with their corresponding chi-square values which are displayed in

TABLE 1 Determination of parameters D_e (eV) and b (\AA^{-1}) keeping R_e (= 1.27455 \AA) as constant, for reducing interval sizes

Interval	No. of iterations	Old parameters		New parameters		χ^2
		D_e	b	D_e	b	
(-0.1,0.1)	20000	5	1	5.346809	1.735122	0.022031
(-0.01,0.01)	10000	5.346809	1.735122	5.346446	1.735122	0.079440
(-0.001,0.001)	10000	5.346446	1.735122	5.346853	1.735120	0.021558
(-0.0001,0.0001)	10000	5.346853	1.735120	5.346953	1.735102	0.021375
(-0.00001,0.00001)	10000	5.346953	1.735102	5.347819	1.734941	0.019944

TABLE 2 Final optimized Morse potential parameters D_e (eV), b (\AA^{-1}) and R_e (\AA) obtained using VMC for five different runs:

Sr. No.	D_e	b	R_e	χ^2 -value
1	5.348363	1.734841	1.274187	0.019219
2	5.353239	1.733939	1.264900	0.018536
3	5.353913	1.733814	1.274379	0.019265
4	5.353953	1.733807	1.274438	0.019315
5	5.352160	1.734139	1.274553	0.017783

Table 2. Even though, one could take mean of the obtained values and determine the uncertainty, it is best to consider the parameter values as those for which minimum χ^2 -value has been obtained.

When number of decimal places in final parameter values obtained was rounded to five, four and three places, the χ^2 -value is obtained as 0.0178044, 0.0281803 and 0.319032 respectively. Hence, six decimal places are retained for performing further calculations.

4.1 | Ro-vibrational spectrum of HCl

To validate the goodness of fit of model parameters obtained using VMC, the study of rotation-vibration spectra of HCl molecule has been undertaken for obtaining the rotational fine structure in the fundamental transition. To accomplish this, effect of rotation due to presence of centrifugal term needs to be included in solving the TISE in Eq. (8). Even though, for each J -value, one will obtain many vibrational states, only the first two energy values corresponding to $v = 0$ and $v = 1$ are recorded as shown in Table 3. Using selection rule $\Delta J = J' - J'' = \pm 1$, differences in energies are accordingly taken to obtain R- and P- branch lines respectively as shown in columns 4 and 5 of Table 3. The same lines are also obtained using analytical expressions as discussed below.

Analytical treatment: For $\Delta J = J' - J'' = +1$ in Eq. (15), we obtain R- branch lines with wavenumbers given by

$$\bar{\nu}_R = \bar{\omega}_0 + (B_1 + B_0)(J'' + 1) + (B_1 - B_0)(J'' + 1)^2 \quad (30)$$

where lower rotational quantum number, $J'' = 0, 1, 2, 3, \dots$

and for getting P-branch lines, substitute $\Delta J = J' - J'' = -1$ in Eq. (15) with wavenumbers

$$\bar{\nu}_R = \bar{\omega}_0 - (B_1 + B_0)(J' + 1) + (B_1 - B_0)(J' + 1)^2 \quad (31)$$

where $J' = 0, 1, 2, 3, \dots$. Also, rotational constant, B corresponding to the vibrational state ν is given by

$$B_\nu = B_e - \beta_e(\nu + 1/2) \quad (32)$$

where β_e reflects how rotational constant B varies with vibrational quantum number ν . So, for $\nu = 0$ state,

$$B_0 = B_e - \frac{1}{2}\beta_e$$

and for $\nu = 1$ state

$$B_1 = B_e - \frac{3}{2}\beta_e \quad (33)$$

Using the values of $\beta_e = 0.30167 \text{ cm}^{-1}$, $B_e = 10.58919 \text{ cm}^{-1}$ from multiple regression data[?] and substituting in above equations, B_0 and B_1 are obtained as $10.438355 \text{ cm}^{-1}$ and $10.136685 \text{ cm}^{-1}$ respectively. Now, putting these values in Eqs. (30) and (31), wavenumbers corresponding to R-branch and P-branch lines are calculated which are shown in column 6 and 7 of Table 3 respectively. In the final two columns, the experimental data recorded using a Nicolet 730 FTIR spectrometer is shown. Since, the experimental results are available to 3 decimal places, accordingly the simulation and analytical outcomes are rounded to 3 decimal places as well.

From Table 3, one can observe that results obtained through simulation by optimizing the potential parameters through VMC are better than those obtained from analytical technique using multiple regression data, as these values are much closer to experimental ones.

4.2 | Comparative analysis of Matrix method with NU and AIM methods:

While experimentally only frequencies are available, analytical and numerical solutions result in the bound state energy levels, from which one obtains the transition frequencies. So as to check the effectiveness of matrix methods based numerical technique that has been implemented in this paper, a comparative study has been undertaken with two analytical techniques. The rotational energy levels for each of the first three vibrational levels are obtained by choosing the optimized Morse potential model parameters using VMC that resulted in minimum χ^2 - value, as given in Table 2. The energy eigen values so obtained are compared with analytical results determined explicitly from approximate techniques of Nikiforov-Uvarov(NU) and Asymptotic Iteration method(AIM).

The analytical expression to determine energy values through NU method (Berkdemir 2005) is given as

$$E_{nJ} = \frac{J(J+1)\hbar^2}{2\mu R_e^2} \left(1 - \frac{3}{a_0} + \frac{3}{a^2 R_e^2}\right) - \frac{\hbar^2 a^2}{2\mu} \left[\frac{e_2}{2\sqrt{e_3}} - \left(n + \frac{1}{2}\right) \right]^2 \quad (34)$$

TABLE 3 Comparative validation of simulated P- and R-branch lines corresponding to fundamental vibrational band in fine-spectrum of HCl molecule with those obtained using analytical and experimental techniques

J''	$\epsilon_{J'',v''=0}$	$\epsilon_{J'',v''=1}$	Simulation(MM)		Analytical(Regression)		Experiment(FTIR)	
			$\bar{\nu}_R(cm^{-1})$	$\bar{\nu}_P(cm^{-1})$	$\bar{\nu}_R(cm^{-1})$	$\bar{\nu}_P(cm^{-1})$	$\bar{\nu}_R(cm^{-1})$	$\bar{\nu}_P(cm^{-1})$
0	-41686.3551	-38800.5308	2906.185	2864.913	2906.566	2865.416	2905.995	2864.834
1	-41665.4436	-38780.1701	2925.983	2843.462	2928.046	2845.746	2925.581	2843.315
2	-41623.6326	-38739.4601	2945.205	2821.489	2950.129	2826.679	2944.577	2821.249
3	-41560.9488	-38678.4273	2963.839	2799.002	2799.002	2808.2156	2962.955	2798.641
4	-41477.4293	-38597.1097	2981.870	2776.016	2996.106	2790.356	2980.689	2775.499
5	-41373.1257	-38495.5589	2999.288	2752.543	3019.999	2773.099	2997.788	2751.817
6	-41248.1017	-38373.8377	3016.078	2728.595	3044.496	2756.446	3014.202	2727.624
7	-41102.4331	-38232.0237	3032.228	2704.185	3069.596	2740.396	3029.941	2702.907
8	-40936.2087	-38070.2054	3047.726	2679.324	3095.300	2724.949	3044.965	2677.697
9	-40749.5293	-37888.4831	3062.558	2654.025	3121.606	2710.106	3059.234	2651.932
10	-40542.5085	-37686.9711	3076.713	2628.300	3148.517	2695.866	3072.771	2625.689
11	-40315.2715	-37465.7953						

TABLE 4 Comparison of bound state energy eigen values of HCl molecule for Morse potential obtained by matrix method with those from NU and AIM methods

Energy values(eV)				
	J	MM	NU	AIM
$v = 0$	0	-5.1684	-5.1684	-5.1684
	5	-5.1296	-5.1296	-5.1296
	10	-5.0266	-5.0266	-5.0266
$v = 1$	0	-4.8106	-4.8106	-4.8106
	5	-4.7728	-4.7728	-4.7728
	10	-4.6726	-4.6725	-4.6725
$v = 2$	0	-4.4657	-4.4657	-4.4657
	5	-4.4289	-4.4289	-4.4289
	10	-4.3314	-4.3313	-4.3313

where

$$\frac{\epsilon_2}{2\sqrt{\epsilon_3}} = \frac{1}{b^2\sqrt{\epsilon_3}} \left[\frac{2\mu D_e}{\hbar^2} - \frac{J(J+1)}{R_e^2} \frac{\epsilon_2}{2\sqrt{\epsilon_3}} \left(\frac{2}{bR_e} - \frac{3}{b^2 R_e^2} \right) \right] \quad (35)$$

$$\epsilon_3 = \frac{2\mu R_e^2 (D_e + \gamma D_2)}{\hbar^2 \alpha^2}; D_2 = \frac{-1}{\alpha} + \frac{3}{\alpha^2} \quad \text{and} \quad \alpha = bR_e \quad (36)$$

and using AIM, analytical expression (Bayrak 2006) is

$$E_{nJ} = \frac{\hbar^2}{2\mu R_e^2} \left[\frac{\beta_1^2}{2\beta_2} - \left(n + \frac{1}{2} \right) \alpha \right] + \gamma c_0 \quad (37)$$

where

$$\beta_1^2 = \frac{2\mu R_e^2}{\hbar^2} (2D_e - \gamma c_1); \quad \beta_2^2 = \frac{2\mu R_e^2}{\hbar^2} (\gamma c_2 + 2D_e) \quad (38)$$

and $c_0 = 1 - \frac{3}{\alpha} + \frac{3}{\alpha^2}$; $c_1 = \frac{4}{\alpha} - \frac{6}{\alpha^2}$; $c_2 = \frac{-1}{\alpha} + \frac{3}{\alpha^2}$; and $\gamma = \frac{J(J+1)\hbar^2}{2\mu R_e^2}$.

In Table 4, comparison of energy levels has been made between matrix method(MM), NU and AIM techniques for $J = 0, 5$ and 10 values, for $v = 0, 1$ and 2 values. It can be seen that the results obtained by matrix method are in good agreement with those obtained from AIM and NU methods up to four decimal accuracy in the vibrational ground state. A small variation of 1 unit in the fourth decimal place could be observed for $J = 10$ values in first and second excited vibrational states in comparison to the analytical results.

5 | CONCLUSION:

The matrix methods numerical technique has been implemented to solve the Schrodinger equation for Morse potential. The vibrational frequencies of HCl, obtained from simulation are matched with the experimental ones in the least square sense by minimizing χ^2 -value using variational Monte-Carlo approach for the first time. The best optimized model parameters obtained within few runs of VMC algorithm are $D_e = 5.352160eV$, $b = 1.734139\text{\AA}^{-1}$ and $R_e = 1.274553\text{\AA}$. These are utilised for determining the spectral lines in the rotational fine structure of HCl and are found to be matching with experimental data better than those resulting from analytical expressions fitted using multiple regression analysis. The energies obtained from simulation match very well with those resulting from analytical expressions of NU and AIM methods confirming the effectiveness of the numerical technique implemented.

References

- Modified Rosen-Morse potential-energy model for diatomic molecules.* (2012). *Physical Review A*, 86.
- Approximate solutions of the Dirac equation for the Rosen-Morse potential including the Spin-orbit centrifugal term.* (2010). *Journal of Mathematical Physics*, 51.
- Minutes of the Middletown meeting, October 14, 1933.* (1933). *Physical Review*, 44
- Exact solutions of the Schrödinger equation.* (1935). *Physical Review*, 48
- Analytical approximations to the solutions of the Manning-Rosen potential with centrifugal term.* (2007). *Physics Letters A*, 368.
- Approximate l-state solutions of the D-dimensional Schrödinger equation for Manning-Rosen potential.* (2008). *Annalen der Physik*, 17.
- Bound state solutions of the Schrödinger equation for modified Kratzer's molecular potential.* (2006). *Chemical Physics Letters*, 417.
- Relativistic treatment of a spin-zero particle subject to a Kratzer-type potential," American Journal of Physics.* (2007). *American Journal of Physics*, 75.
- Exact solutions of the radial Schrödinger equation for some physical potentials.* (2008). *Central European Journal of Physics*, 6.
- Exact solutions of the Schrodinger equation for the deformed hyperbolic potential well and the deformed four-parameter exponential type potential.* (2000). *Physics Letters A*, 275
- Mapping of the five-parameter exponential-type potential model into trigonometric-type potentials.* (2004). *Journal of Physics A*, 37.
- On the vibrations of polyatomic molecules.* (1932). *Physical Review*, 42.
- On some exactly solvable potentials derived from supersymmetric quantum mechanics.* (1992). *Journal of Physics A*, 25.
- Supersymmetric improvement of the Pekeris approximation for the rotating Morse potential.* (2004). *Chemical physics letters*, 394.
- Exact solutions of the modified Kratzer potential plus ring-shaped potential in the D-dimensional Schrödinger equation by the Nikiforov-Uvarov method.* (2008). *International Journal of Modern Physics C*, 19.
- Special functions of mathematical physics.* (1988). Basel: Birkhäuser.
- Rotational correction on the Morse potential through the Pekeris approximation and Nikiforov-Uvarov method.* (2005). *arXiv preprint quant-ph/0502182*.

Mapping of shape invariant potentials under point canonical transformations. (1992). *Journal of Physics A: Mathematical and General*. 25.

Approximate solutions of the Schrödinger equation with the generalized Morse potential model including the centrifugal term. (2011). *International Journal of Quantum Chemistry*. 111.

Applications of automatic differentiation to the time-dependent Schrödinger equation. (2011). *International Journal of Quantum Chemistry*. 111.

On the time-dependent solutions of the Schrödinger equation. I. The linear time-dependent potential. (2011). *International Journal of Quantum Chemistry*. 111.

Morse potential eigen-energies through the asymptotic iteration method. (2007). *International Journal of Quantum Chemistry*. 107.

Arbitrary l-state solutions of the rotating Morse potential through the exact quantization. (2007). *Physics Letters A*. 363.

Bc meson spectrum and hyperfine splittings in the shifted large-N- expansion technique. (2003). *International Journal of Modern Physics A*. 18.

Solving the vibrational Schrödinger equation on an arbitrary multidimensional potential energy surface by the finite element method. (2009). *Computer Physics Communications*. 180.

Comparison of some special optimized fourth-order Runge-Kutta methods for the numerical solution of the Schrödinger equation. (2005). *Computer physics communications*. 166.

Trigonometrically fitted fifth-order runge-kutta methods for the numerical solution of the schrödinger equation. (2005). *Mathematical and computer modelling*. 42.

Explicit series solutions of some linear and nonlinear Schrodinger equations via the homotopy analysis method. (2009). *Communications in Nonlinear Science and Numerical Simulation*. 14.

Approximate solution for the Klein-Gordon-Schrödinger equation by the homotopy analysis method. (2010). *Chinese Physics B*. 19.

Approximate analytical versus numerical solutions of Schrödinger equation under molecular Hua potential. (2012). *International Journal of Quantum Chemistry*. 112.

Bound State Solutions of D-Dimensional Schrodinger Equation with Exponential-Type Potentials. (2014). *International Journal of Quantum Chemistry*. 115.

The harmonic oscillator in quantum mechanics: A third way. (2009). *American Journal of Physics*. 77.

Solving for three-dimensional central potentials using numerical matrix methods. (2009). *American Journal of Physics*. 81.

Simulation study of nuclear shell model using sine basis. (2020). *American Journal of Physics*. 88.

Numerical simulation of quantum anharmonic oscillator, embedded within an infinite square well potential, by matrix methods using gnumeric spreadsheet. (2020). *American Journal of Physics*. 41.

[Colin N Banwell] *Fundamentals of molecular spectroscopy*. (1972). McGraw-Hill, New York.

Analysis of the infrared spectra of diatomic molecules. (1999). *Journal of Chemical Education*, 76.

Fundamentals of molecular spectroscopy. (1989). John Wiley and Sons, New York.

Diatomic molecules according to the wave mechanics. II. Vibrational levels. (1929). *Phys. Rev.*, 34. Asymmetric wave functions from tiny perturbations. (2015). *Am. J. Phys.*, 83.

Numerical matrix method for quantum periodic potentials. (2016). *Am. J. Phys.*, 84. *Molecular spectra and molecular structure: IV. Constants of diatomic molecules*. (2013). *Spectra of atoms and molecules*. (2020). Oxford university press.

Modified Rosen-Morse potential-energy model for diatomic molecules. (2012). *Physical Review A*, 86.

Rotational correction on the Morse potential through the Pekeris approximation and Nikiforov-Uvarov method. (2005). *ArXiv Preprint Quant-Ph/0502182*.

Arbitrary l-state solutions of the rotating Morse potential by the asymptotic iteration method. (2006). *Journal of Physics A: Mathematical and General*, 39.

Simulation of Vibrational Spectrum of Diatomic Molecules Using Morse Potential by Matrix Methods in Gnumeric Worksheet. (2020). *Physics Education*.

Numerical Solution of Square Well Potential With Matrix Method Using Worksheets. (2019). *Physics Education*, 36.